Synthetase Recognition Determinants of *E. coli* Valine Transfer RNA†

Jack Horowitz,* Wen-Chy Chu,‡ Wesley B. Derrick,§ Jack C.-H. Liu,|| Mingsong Liu,⊥ and Dongxian Yue#

Department of Biochemistry, Biophysics, and Molecular Biology, Iowa State University, Ames, Iowa 50011

Received March 2, 1999; Revised Manuscript Received April 19, 1999

ABSTRACT: We have studied the interactions between *Escherichia coli* $tRNA^{Val}$ and valyl-tRNA synthetase (ValRS) by enzymatic footprinting with nuclease S1 and ribonuclease V1, and by analysis of the aminoacylation kinetics of mutant $tRNA^{Val}$ transcripts. Valyl-tRNA synthetase specifically protects the anticodon loop, the 3′ side of the stacked T-stem/acceptor-stem helix, and the 5′ side of the anticodon stem of $tRNA^{Val}$ against cleavage by double- and single-strand-specific nucleases. Increased nuclease susceptibility at the ends of the anticodon- and T-stems in the $tRNA^{Val}$•ValRS complex is indicative of enzyme-induced conformational changes in the tRNA. The most important synthetase recognition determinants are the middle and 3′ anticodon nucleotides (A35 and C36, respectively); G20, in the variable pocket, and G45, in the tRNA central core, are minor recognition elements. The discriminator base, position 73, and the anticodon stem also are recognized by ValRS. Replacing wild-type A73 with G73 reduces the aminoacylation efficiency more than 40-fold. However, the C73 and U73 mutants remain good substrates for ValRS, suggesting that guanosine at position 73 acts as a negative determinant. The amino acid acceptor arm of $tRNA^{Val}$ contains no other synthetase recognition nucleotides, but regular A-type RNA helix geometry in the acceptor stem is essential [Liu, M., et al. (1997) *Nucleic Acids Res. 25*, 4883−4890]. In the anticodon stem, converting the U29:A41 base pair to C29:G41 reduces the aminoacylation efficiency 50-fold. This is apparently due to the rigidity of the anticodon stem caused by the presence of five consecutive C:G base pairs, since the A29:U41 mutant is readily aminoacylated. Identity switch experiments provide additional evidence for a role of the anticodon stem in synthetase recognition. The valine recognition determinants, A35, C36, A73, G20, G45, and a regular A-RNA acceptor helix are insufficient to transform *E. coli* $tRNA^{Phe}$ into an effective valine acceptor. Replacing the anticodon stem of $tRNA^{Phe}$ with that of $tRNA^{Val}$, however, converts the tRNA into a good substrate for ValRS. These experiments confirm G45 as a minor ValRS recognition element.

The ability of aminoacyl-tRNA synthetases to discriminate their cognate tRNA(s) from structurally similar noncognate species is crucial for maintaining translational fidelity. This specificity depends on recognition by the enzyme of a defined set of nucleotides and structural features that determine tRNA identity. Much progress has recently been made in identifying synthetase recognition determinants, both those required for efficient aminoacylation (positive determinants) and those that prevent productive recognition of noncognate tRNAs (negative determinants), for each of the 20 isoaccepting tRNA groups in *E. coli* (reviewed in *1*−*4*). Relatively few nucleotides in tRNA contribute to recognition, and these are scattered throughout the three-dimensional structure of the molecule, with a different distribution in different tRNAs. Positive recognition elements are found in the anticodon of all *E. coli* tRNAs, except those for serine, alanine, and leucine (17 out of 20) (*5*). The discriminator base (position 73), the most distal base pairs of the acceptor stem, the variable pocket (formed by nucleotides 16, 17, 20, 59, and 60), and less frequently the variable loop and the augmented D-helix also contain recognition elements for many synthetases (*1, 2, 4, 6*), as do certain posttranscriptionally modified nucleotides in the anticodon loop (*7, 8*). Crystallographic (*9, 10*) and chemical footprinting studies (*11*) have revealed that recognition elements either are in direct contact with the synthetase or affect the presentation of the contact nucleotides to the synthetase by influencing tRNA structure (*2*−*4, 12*−*14*).

The idiosyncratic nature of synthetase−tRNA interactions underlines the need for detailed structural information of additional tRNA−synthetase complexes. In this paper we describe nuclease footprinting experiments that identify sites on $tRNA^{Val}$ that interact directly with *E. coli* valyl-tRNA synthetase (ValRS),[1] and report a detailed analysis of the aminoacylation kinetics of mutant *E. coli* $tRNA^{Val}$ transcripts to determine the synthetase recognition determinants for

† This work was supported in part by Grant MCB 95-13932 from the National Science Foundation (J.H.). This is Journal Paper No. J-18289 of the Iowa Agriculture and Home Economics Experiment Station, Ames, IA, Project No. 3552.

* To whom correspondence should be addressed at the Department of Biochemistry, Biophysics, and Molecular Biology, 4116 Molecular Biology Building, Iowa State University, Ames, IA 50011. Phone: (515) 294-8344. FAX: (515) 294-0453. E-mail: jhoro@iastate.edu.

‡ Present address: Research and Product Development, Pioneer Hi-Bred International, Johnston, IA 50131.

§ Present address: Department of Chemistry and Biochemistry, University of Colorado at Boulder, Boulder, CO 80309.

|| Present address: College of Dentistry, University of Iowa, Iowa City, IA 52242.

⊥ Present address: Cardiovascular Research Institute, University of California, San Francisco, San Francisco, CA 94143.

Present address: Ambion, Inc., Austin, TX 78744.

10.1021/bi990490b CCC: $18.00
Published on Web 05/26/1999

aminoacylation of this tRNA. Although the major synthetase recognition elements of $tRNA^{Val}$ are located in the anticodon (*15*−*18*), nucleotides in other parts of the tRNA and structural features of the molecule also contribute to the specificity of synthetase recognition. Preliminary accounts of some of these results have appeared (*16, 19*).

MATERIALS AND METHODS

Materials. Native $tRNA^{Val}$(UAC) (1600 pmol/A_{260}) was purchased from Subriden RNA, and further purified by denaturing gel electrophoresis. Ribonuclease T1 was purchased from Boehringer Mannheim. Nuclease S1 and ribonuclease V1, both FPLC-pure grade enzymes, were from Pharmacia/LKB. Ribonuclease-free, molecular biology grade, bovine serum albumin was purchased from Boehringer Mannheim. Nucleoside triphosphates (ATP, CTP, GTP, and UTP) were products of the United States Biochemical Corp. 5-Fluorouridine 5′-triphosphate (FUTP) was prepared by Sierra Bioresearch. T7 RNA polymerase was isolated from *E. coli* BL21/pAR1219 as reported by Zawadzki and Gross (*20*). Homogeneous valyl-tRNA synthetase was prepared from *E. coli* GRB238/pHOV1 as described by Chu and Horowitz (*21*), and *E. coli* phenylalanyl-tRNA synthetase was partially purified as described by Peterson and Uhlenbeck (*22*).

Preparation of tRNA. DNA templates for in vitro transcription by T7 RNA polymerase were derived from the recombinant phagemid pVAL119-21, containing the cloned wild-type *E. coli* $tRNA^{Val}$ gene linked to an upstream bacteriophage T7 promoter, as reported previously (*23*). pFPHE119 is a similar construct containing the *E. coli* $tRNA^{Phe}$ gene, and was prepared (Liu and Horowitz, unpublished) from recombinant pUS618 (*22*) containing the $tRNA^{Phe}$ gene, kindly supplied by Dr. O. C. Uhlenbeck (University of Colorado, Boulder). The $tRNA^{Phe}$ gene sequence differs from that of natural $tRNA^{Phe}$ by having the C3:G70 base pair replaced by G3:C70 to improve transcription efficiency (*22*). Mutations were introduced into the cloned tRNA genes by site-directed mutagenesis (*24*) using mutagenic oligonucleotides synthesized by the Nucleic Acid Facility at Iowa State University. Mutants were selected by dideoxy DNA sequence analysis (*25*).

Transfer RNAs were transcribed in vitro from the synthetic tRNA genes as described (*26*). The transcripts, purified by HPLC (*27*), could be aminoacylated to levels of 1100−1500 pmol/A_{260}, unless otherwise indicated. Both native and in vitro transcribed $tRNA^{Val}$ were quantified by spectrophotometric measurements at 260 nm, assuming a value of $E_{260}^{0.1\%} = 24$.

Nuclease Mapping. Contacts between ValRS and *E. coli* $tRNA^{Val}$ were mapped by enzymatic probing reactions with nuclease S1 and ribonuclease V1 at pH 7.2 and 5.0; the synthetase binds tRNA more strongly at acidic pH (*28*). For these experiments, transfer RNA was 5′-^{32}P-labeled with T4 polynucleotide kinase (*29*) and purified by gel electrophoresis. Limited hydrolysis of the ^{32}P-end-labeled tRNA (*30*) was carried out at 4 °C for the times indicated, in the presence and absence of added ValRS (4.9−5.3 μM) in reaction mixtures (10 μL) buffered at pH 7.2 (50 mM Tris-HCl) or 5.0 (50 mM NaOAc) and containing 10 mM $MgCl_2$, 1 mM $ZnCl_2$, 2 μM unlabeled *E. coli* tRNA (unfractionated), and 25 units of nuclease S1 or 0.15 unit of RNase V1. Reactions lacking ValRS contained an equivalent amount of bovine serum albumin (BSA) to control for any nonspecific effects of protein on the activity or specificity of the enzymatic probe. BSA does not inhibit nuclease S1 or RNase V1 hydrolysis of $tRNA^{Val}$ under the conditions studied, nor does it alter the sites of cleavage. Incubated control reactions included all ingredients except the enzymes. Reactions were terminated by phenol extraction (2×), the aqueous layer was washed with ether (3×) and heated briefly to drive the ether off, and the reaction products were recovered by ethanol precipitation. Pellets were dried by lyophilization and dissolved in 10 μL of sequencing dye solution (8 M urea, 20 mM EDTA, 0.1% bromophenol blue, and 0.1% xylene cyanol).

5′-^{32}P-labeled tRNA was cleaved under conditions that result in a limited scission of tRNA molecules to minimize secondary cleavages. Primary cleavage sites were identified by digesting tRNA with varying amounts of enzyme (results not shown). Levels of nuclease used in probing reactions were approximately half those that gave rise to the first detectable secondary cleavages. RNA fragments detected under these conditions were considered to arise from primary cleavages, although we cannot entirely exclude the possibility that some cleavage products are derived from secondary cuts without examining results with 3′-^{32}P-labeled tRNA.

^{32}P-labeled nuclease cleavage products were separated by electrophoresis in 15% denaturing polyacrylamide gels (*30*) and were visualized by autoradiography. Assignment of cleavage positions was made by comparison with the known positions of G residues in partial RNase T1 digests of $tRNA^{Val}$, and an alkaline hydrolysis ladder. Partial RNase T1 hydrolysates were prepared by incubating 5′-end-labeled $tRNA^{Val}$ (20 000 cpm) in 20 mM sodium citrate, pH 5.0, 1 mM EDTA, 0.6 mg/mL carrier tRNA, 4.2 M urea, 0.025% bromophenol blue, and 0.025% xylene cyanol, with 5 units of RNase T1 at 65 °C for 5 min (*31*). Alkaline ladders were generated by incubating 10 μg of tRNA (20 000 cpm) in 5 μL of 20 mM sodium bicarbonate, pH 9.5, for 5 min at 90 °C.

Steady-State Aminoacylation Kinetics. The kinetics of aminoacylation were determined at 37 °C as previously described (*32*) in a 60 μL reaction mixture containing 100 mM HEPES, pH 7.50, 15 mM $MgCl_2$, 100 mM KCl, 7 mM ATP, 1 mM DTT, 99 μM L-[^{3}H]valine (5 Ci/mmol, from Amersham, Arlington Heights, IL), and transfer RNA ranging from 0.5 to 4 μM. Reactions were initiated by addition of 1 nM purified valyl-tRNA synthetase. K_m and k_{cat} values were determined by a least-squares fit of the double-reciprocal plot of the data. Under our conditions, the K_m for valine is 43 μM (J. Liu and Horowitz, unpublished), and that for ATP is 1.3 mM (*33*).

^{19}F NMR Spectroscopy. For ^{19}F NMR spectroscopy, 5-fluorouracil-substituted tRNAs were transcribed using FUTP in place of UTP. Transfer RNA samples were dissolved in 111% standard NMR buffer (55.55 mM sodium cacodylate, pH 6.0, 16.66 mM $MgCl_2$, 111 mM NaCl, and

[1] Abbreviations: ValRS, valyl-tRNA synthetase; FUra, 5-fluorouracil; (FUra)$tRNA^{Val}$, 5-fluorouracil-substituted *E. coli* $tRNA^{Val}$; HPLC, high-performance liquid chromatography; NMR, nuclear magnetic resonance; BSA, bovine serum albumin; EDTA, ethylenediaminetetraacetic acid.

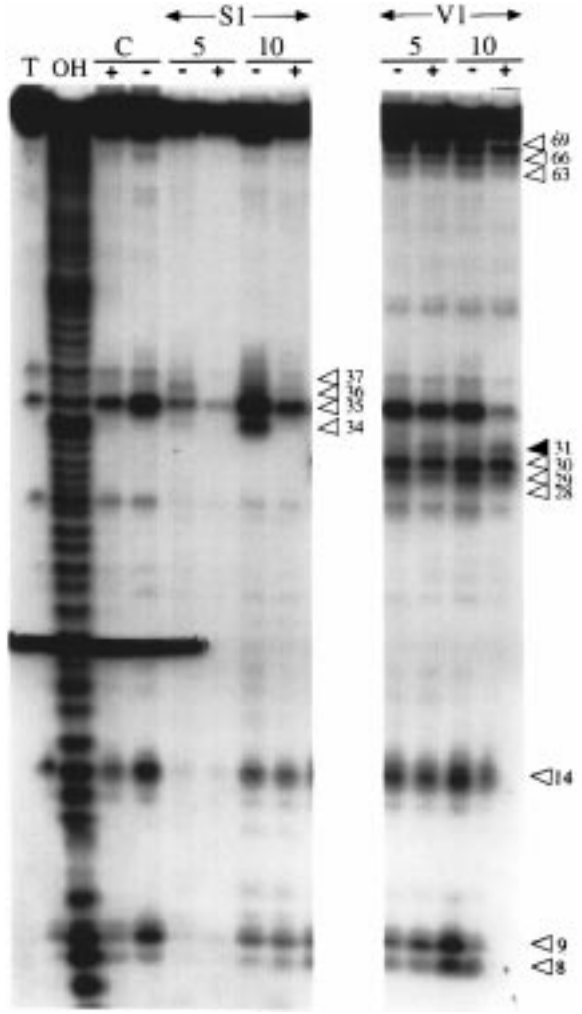

FIGURE 1: Partial nuclease digestion of *E. coli* tRNA^{Val} at pH 7.2 in the presence and absence of ValRS. (T) RNase T1 ladder; (OH) alkaline hydrolysis ladder; (C) incubated control plus and minus ValRS; (S1) nuclease S1 digestion, minus and plus ValRS for 5 min (5) and 10 min (10); (V1) RNase V1 digestion minus and plus ValRS for 5 min (5) and 10 min (10). Open triangles indicate phosphodiester bonds protected from cleavage by ValRS. Solid triangles indicate bonds whose susceptibility to cleavage is increased in the tRNA−ValRS complex.

1.11 mM EDTA) and dialyzed against two changes of the same buffer. Sample volume was adjusted to 450 μL, and 10% (v/v) D_2O was added as an internal lock signal. Before spectra were recorded, tRNA samples were renatured by heating at 55 °C for 20 min, followed by slow cooling to room temperature. ^{19}F NMR spectra were collected at 47 °C on a Varian Unity 500 FT NMR spectrometer at 470 MHz by using 12K data points, with no relaxation delay and a pulse angle optimizing the Ernst condition (*34*).

RESULTS AND DISCUSSION

Nuclease Mapping of Synthetase Contact Sites. Contacts between ValRS and *E. coli* tRNA^{Val} were mapped by nuclease S1 and ribonuclease V1 footprinting, at pH 7.2 and pH 5.0. 5′-^{32}P-end-labeled native (modified) and in vitro transcribed (unmodified) tRNA^{Val} were partially digested with the enzymes in the presence or absence of ValRS (see Materials and Methods). Similar results were obtained for both tRNA samples; only those with native tRNA^{Val} are shown (Figures 1 and 2). Cleavage sites are designated by

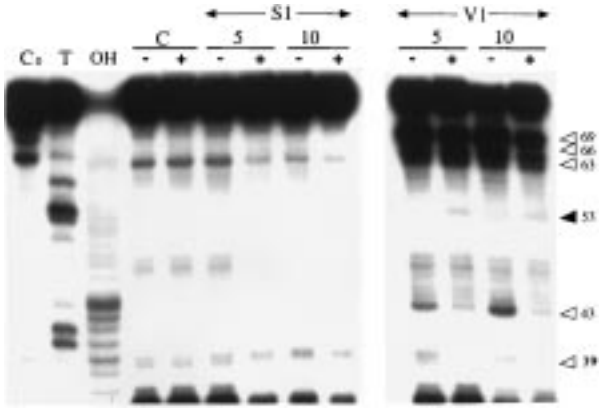

FIGURE 2: Partial nuclease digestion of *E. coli* tRNA^{Val} at pH 5.0 in the presence and absence of ValRS. (C_0) Unincubated control; (T) RNase T1 ladder; (OH) alkaline hydrolysis ladder; (C) incubated control minus and plus ValRS; (S1) nuclease S1 digestion, minus and plus ValRS for 5 min (5) and 10 min (10); (V1) RNase V1 digestion minus and plus ValRS for 5 min (5) and 10 min (10). Symbols and nomenclature are the same as in Figure 1.

the nucleotide that donates the phosphate; i.e., cleavage between the first and second nucleotides from the 5′ end is denoted as cleavage at p2.

At both pH 7.2 and pH 5.0, ValRS protects nucleotides in the anticodon loop of *E. coli* tRNA^{Val}, positions 34−37 (Figure 3a), from nuclease S1 hydrolysis (Figures 1 and 2, left). Cleavage near the 3′-terminus of the tRNA, although unassignable to specific nucleotides, also is significantly reduced by ValRS (Figure 1). Valyl-tRNA synthetase binding to tRNA^{Val} is quite specific. The enzyme does not inhibit cleavage of 5′-^{32}P-labeled *E. coli* tRNA$_m^{Met}$ by nuclease probes (results not shown), this despite the fact that tRNA$_m^{Met}$ can be aminoacylated with valine when the Met anticodon is replaced with that for valine (*15*).

RNase V1 footprinting experiments at pH 7.2 reveal contacts between ValRS and the anticodon stem, the T-stem, and the amino acid acceptor stem of tRNA^{Val} (Figure 1, right). The synthetase protects positions 69 (in the aminoacyl-acceptor stem), 66 (at the junction of the amino acid acceptor and T-stems), 63 (in the T-stem), and 28−30 on the 5′ side of the anticodon stem, from RNase V1 hydrolysis. At pH 5.0, where the synthetase binds tRNA more tightly (*28*), protection at position 69 is more evident, and protection at p43 (in the anticodon arm) is observed (Figure 2, right).

Under conditions of the experiment, spontaneous hydrolysis of tRNA^{Val} occurs, most frequently at labile pyrimidine−adenine phosphodiester linkages (YpA) (*35*), e.g., p9, p14, p26, p35, and p37 (Figures 1 and 2). Valyl-tRNA synthetase protects the tRNA from spontaneous cleavage at positions 8, 9, 14, and 39 (Figures 1 and 2). Results of the nuclease probing experiments are summarized in Figure 3b. It is clear that ValRS makes strong contacts with the anticodon loop, the 5′ side of the anticodon stem, and the 3′ side of the stacked T-stem/acceptor stem helix.

Two phosphodiester bonds at the ends of helical stems of tRNA^{Val} become more susceptible to RNase V1 hydrolysis as a result of ValRS binding: p31, in the anticodon stem (Figure 1, right); and p53, in the T-stem (Figure 2, right). This suggests that conformational changes occur in the anticodon stem and the T stem when the synthetase interacts with tRNA^{Val}. Such changes were detected in ^{19}F NMR

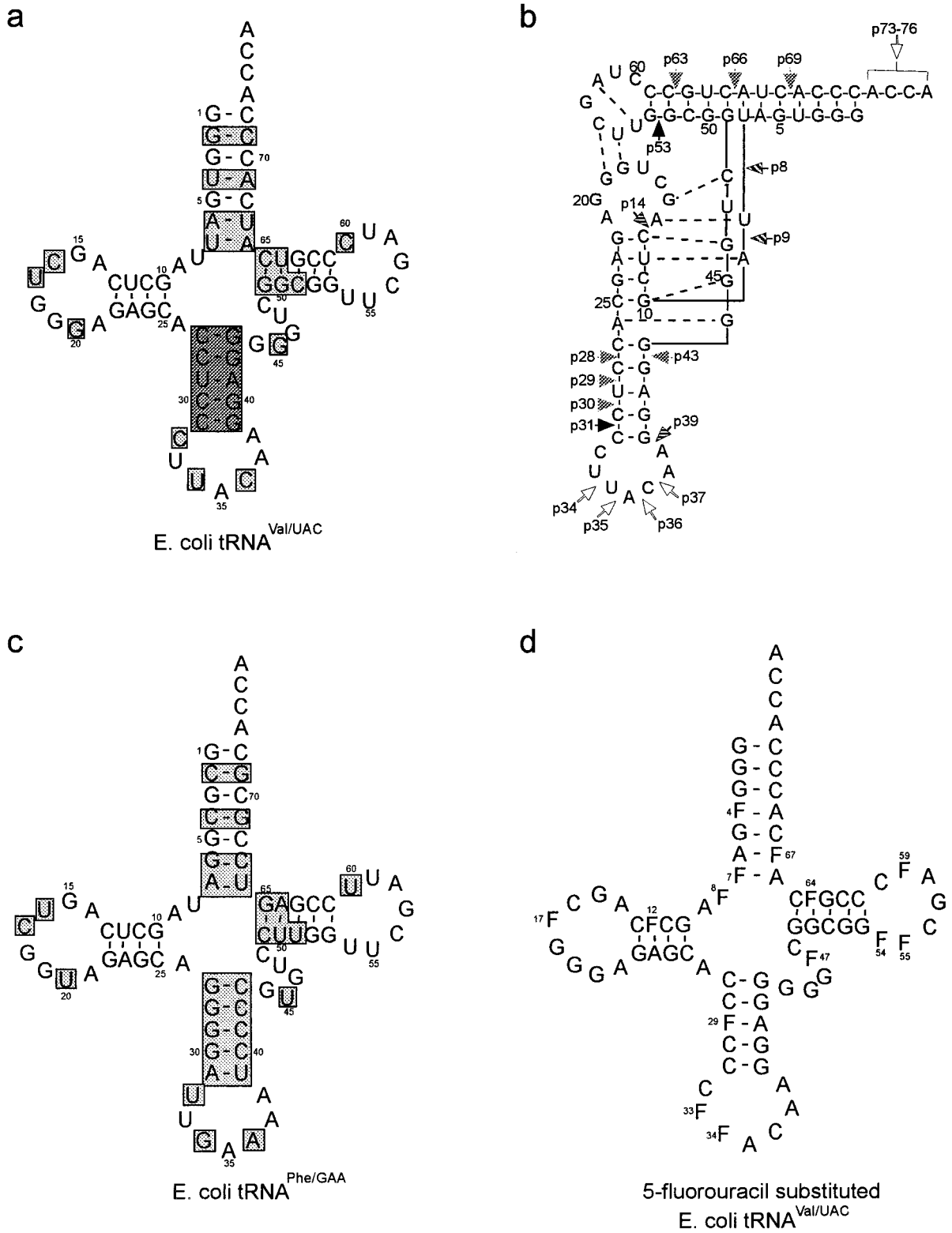

FIGURE 3: Nucleotide sequences of the tRNAs used in these studies: (a) *E. coli* $tRNA^{Val}$. Shaded areas in (a) and (c) indicate sequence differences between *E. coli* $tRNA^{Val}$ and *E. coli* $tRNA^{Phe}$. (b) Summary of nuclease footprinting results shown on the structure of *E. coli* $tRNA^{Val}$. (White arrowhead) Phosphodiester bonds protected from nuclease S1 hydrolysis by ValRS; (stippled arrowhead) bonds protected from RNase V1 hydrolysis by ValRS; (hatched arrowhead) bonds protected by ValRS from spontaneous hydrolysis; (black arrowhead) bonds hydrolyzed more readily by RNase V1 in ValRS-bound $tRNA^{Val}$. (c) *E. coli* $tRNA^{Phe}$ with the natural C3:G70 base pair replaced by G3:C70. (d) 5-Fluorouracil-substituted *E. coli* $tRNA^{Val}$.

experiments with 5-fluorouracil-substituted *E. coli* $tRNA^{Val}$ (*21*). ^{19}F NMR is well suited for monitoring structural changes because of the high resolution of ^{19}F NMR spectra and the sensitivity of the fluorine nucleus to changes in its environment. 5-Fluorouracil-substituted $tRNA^{Val}$ retains full aminoacylation activity, despite replacement of all uracils by the base analogue (*23, 36, 37*). There are 14 fluorouracil residues distributed throughout every stem and loop of the tRNA molecule (Figure 3d). The ^{19}F spectrum of (FUra)-$tRNA^{Val}$ shows a resolved peak for each incorporated FUra

and has been completely assigned (*38, 39*). Comparison of the ^{19}F spectrum of the free tRNA with that of ValRS-bound tRNA^{Val} indicates enzyme binding causes partial unwinding of the T-stem helix near position 64 and a limited disruption of T-loop/D-loop interactions (*21*). This unwinding could account for inhibition of RNase V1 hydrolysis at p63, because the enzyme acts preferentially at helical or base-stacked regions (*40*).

^{19}F NMR also detects the strong interactions of ValRS with the anticodon of tRNA^{Val}. Loss of intensity of the signal from FU34 is the major effect of synthetase binding on the ^{19}F spectrum of (FUra)tRNA^{Val} (*21*). Schweizer and co-workers reported comparable results in ^{13}C NMR experiments probing the interaction of [4,5-^{13}C]uracil-labeled *E. coli* tRNA^{Val} and *B. stearothermophilus* valyl-tRNA synthetase (*41, 42*). ^{19}F NMR experiments also provide evidence for synthetase contacts at FU7 and FU67 (*21*), consistent with the nuclease footprinting results, which show protection by ValRS against nuclease V1 cleavage at the nearby residues 8 and 9 and at 66 (Figures 1 and 2).

Synthetase Recognition Determinants of tRNA^{Val}. Unmodified wild-type tRNA^{Val} transcripts exhibit nearly the same aminoacylation kinetics as native (modified) tRNA^{Val} (*23*). This allows us to identify nucleotides and structural features of the tRNA that serve as ValRS recognition determinants, by analysis of the steady-state aminoacylation kinetics of in vitro transcribed tRNA^{Val} mutants. Mutations were introduced in all parts of the tRNA^{Val} molecule, particularly those shown by nuclease footprinting to be contacted by ValRS.

(1) Anticodon Loop. Nuclease footprinting experiments identify the anticodon as a key site of ValRS interaction with tRNA^{Val} (Figure 1). Schulman and co-workers initially reported (*15, 17, 43*) that the anticodon is the main synthetase recognition determinant of tRNA^{Val} (also see refs *16, 18*). To determine the quantitative contribution to synthetase recognition of individual positions in the anticodon, the aminoacylation kinetics of anticodon mutants of tRNA^{Val} were analyzed. The results (Table 1) identify A35 and C36 as major synthetase recognition determinants. Mutants at position 35 are aminoacylated only 10^{-5} as efficiently as wild-type tRNA^{Val}, and those at position 36 are 2−3 orders of magnitude less active. Mutants at position 34, however, remain good substrates for ValRS, as expected, because *E. coli* valine isoaccepting tRNAs have either a G or a U at position 34. Substituting A36 for the wild-type C36 is less deleterious than replacing C36 with U36 or G36 (Table 1), suggesting that the exocyclic 4- or 6-NH functional group of C or A is recognized by ValRS.

Efficient binding of tRNA^{Val} to ValRS requires an unaltered valine anticodon; anticodon mutants have a low affinity for the enzyme. This is exemplified by the failure of mutant G35 to inhibit aminoacylation of wild-type tRNA^{Val} (2 μM) at concentrations up to 6 μM (Figure 4a). A truncated tRNA^{Val} missing the single-stranded 3′-terminal ACCA sequence, but retaining the wild-type anticodon, readily inhibits the aminoacylation reaction (Figure 4a).

ValRS recognizes the valine anticodon sequence even when it is displaced from its usual position in the anticodon loop. The A35U and C36A anticodon mutants of tRNA^{Val} are each 3−5 orders of magnitude less efficient as substrates for ValRS than the wild-type tRNA (Table 1), and the double mutant A35U;C36A (which retains the wild-type A37) has no detectable aminoacylation activity (Figure 4b). However, when A37 in the double mutant is converted to C37, introducing the valine anticodon sequence shifted one position toward the 3′ side of the anticodon loop (U35A36C37), the tRNA readily accepts valine, although at a slower rate than wild-type tRNA^{Val}; its charging level almost reaches that of the wild-type tRNA after 1 h (Figure 4b). The mutant tRNA^{Val} with the anticodon sequence shifted one position to the 5′ side of the anticodon loop (U33A34C35) has no detectable aminoacylation activity (results not shown), presumably because of the sharp U-turn in the anticodon loop between nucleotides 33 and 34.

Table 1: Aminoacylation Kinetics of Anticodon Arm Mutants of *E. coli* tRNA^{Val}

tRNA	K_m (μM)	k_{cat} (s^{-1})	k_{cat}/K_m	relative k_{cat}/K_m
wild-type	1.4	9.0	6.4	(1.0)
anticodon				
U34 → G34	1.9	7.7	4.1	0.63
→ C34	1.7	7.0	4.1	0.63
A35 → G35	–	–	4.9×10^{-5}	7.5×10^{-6}
→ C35	–	–	1.8×10^{-5}	2.8×10^{-6}
→ U35	–	–	5.8×10^{-5}	8.9×10^{-6}
C36 → A36	9.7	0.36	4.0×10^{-2}	5.8×10^{-3}
→ U36	45.9	0.25	5.5×10^{-3}	9.0×10^{-4}
→ G36	46.2	0.40	8.7×10^{-3}	1.3×10^{-3}
anticodon loop				
C32 → U32	1.4	7.2	5.1	0.80
→ G32	0.69	6.5	9.4	1.5
→ A32	0.69	8.1	11.7	1.8
U33 → C33	1.3	8.6	6.6	1.0
→ G33	1.6	10.3	6.4	1.0
A37 → U37	1.1	8.1	7.4	1.2
→ G37	0.99	10.1	10.2	1.6
A38 → G38	4.7	2.5	0.54	8.4×10^{-2}
→ C38	1.4	7.6	5.4	0.84
→ U38	0.45	1.7	3.7	0.58
C32;A38 → G32;C38	2.6	11.9	4.6	0.72
anticodon stem				
U29:A41 → C29:G41	25.1	3.8	0.15	2.3×10^{-2}
→ A29:U41	2.4	9.2	3.8	0.60
C30:G40 → U30:A40	2.0	10.1	5.0	0.78

Effects of mutations at other positions in the anticodon loop of tRNA^{Val} on aminoacylation are summarized in Table 1. Substitutions for C32, U33, and A37 have little effect on general aminoacylation effectiveness (Table 1). The specificity constants (k_{cat}/K_m) of these tRNA^{Val} variants are close to or greater than that of wild-type tRNA^{Val}. Mutant tRNAs with purines at position 32 generally have small K_ms, and relative specificity constants that are greater than 1. Replacing A38 with U lowers both K_m and k_{cat}, but has little effect on the overall aminoacylation efficiency (Table 1); substitution of A38 with C decreases valine acceptance only slightly. However, changing A38 to G38 reduces the specificity constant 12-fold, due to an increase in K_m and a decrease in k_{cat} (Table 1). This could be the result of base pair formation between G38 and C32 at the top of the anticodon loop, extending the RNA helix of the anticodon stem. Extra cross-loop base pairs have been observed in the complex of glutaminyl tRNA with its cognate synthetase, GlnRS, and their formation produces changes in anticodon loop conformation (*44*). Structural changes in the anticodon of the A38G mutant of tRNA^{Val} could inhibit aminoacylation by altering the presentation of the synthetase recognition nucleotides in the anticodon (A35 and C36) to ValRS. Spectral shift

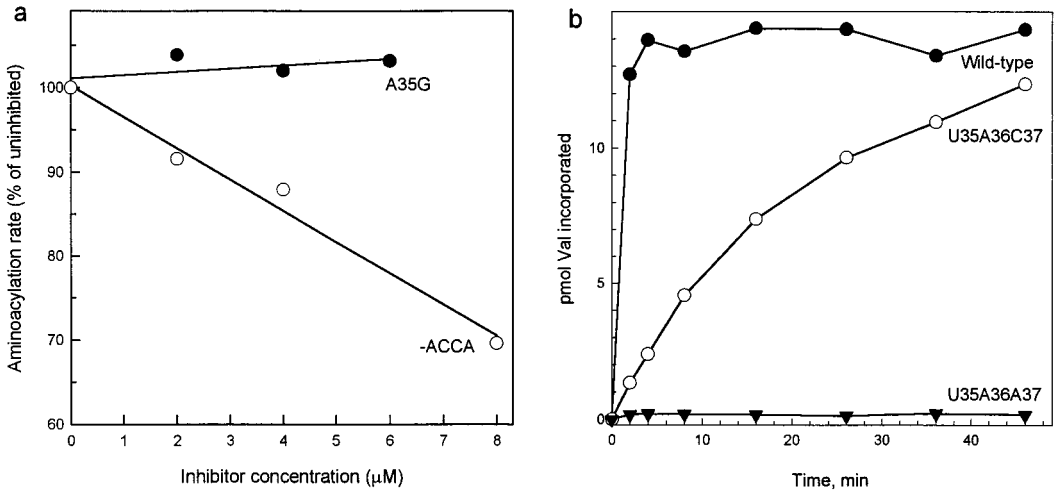

FIGURE 4: (a) Inhibition of wild-type tRNA^{Val} (2 μM) aminoacylation by tRNA^{Val} variants: (●) mutant A35G; (○) mutant lacking 3′-ACCA. (b) Aminoacylation of anticodon mutants of tRNA^{Val}: (●) wild-type; (○) mutant U35A36C37; (▼) mutant U35A36A37.

changes in the ^{1}H NMR and ^{19}F NMR spectra of the A38G mutant of tRNA^{Val} (unpublished results) provide evidence for conformational changes resulting from the transformation of A38 to G38. It is interesting to note that the C32G;A38C double mutant, in which a putative G:C base pair at the top of the anticodon loop would have the opposite orientation, is quite readily aminoacylated (relative $k_{cat}/K_m = 0.72$) (Table 1).

(2) Anticodon Stem. The 5′ side of the anticodon stem contacts ValRS directly (Figures 1 and 2). Results of a mutational analysis of several base pairs in the anticodon stem are presented in Table 1. Conversion of C30:G40 to U30:A40 has little effect on aminoacylation efficiency (Table 1). However, mutating U29:A41 to C29:G41 reduces the charging efficiency 45-fold (Table 1), primarily due to an 18-fold increase in K_m. Although this may result from loss of a direct synthetase recognition site, it is more likely due to the rigidity or lack of flexibility of the anticodon stem caused by the presence of five consecutive C:G base pairs. Replacing U29:A41 with A29:U41 generates a much more active tRNA, having a catalytic efficiency 60% that of wild-type tRNA^{Val} (Table 1). Moreover, ^{19}F NMR experiments show a conformational change in the anticodon loop of the C29:G41 mutant of tRNA^{Val} (*38*), and this may interfere with effective synthetase recognition of the tRNA by altering access of the enzyme to essential functional groups on A35 and C36.

(3) Acceptor Stem. Although ValRS makes direct contact with the acceptor stem of tRNA^{Val}, particularly near p69 (Figure 1), we previously demonstrated the absence of essential recognition nucleotides in the acceptor helix (*45*). Replacing any base pair in the acceptor stem with another Watson−Crick base pair has little effect on aminoacylation efficiency. In addition, *Bacillus stearothermophilus* tRNA^{Val} is readily and fully aminoacylated by *E. coli* ValRS despite major acceptor stem sequence differences from *E. coli* tRNA^{Val} (Tardif and Horowitz, unpublished). Moreover, *E. coli* tRNA^{Ala} and yeast tRNA^{Phe}, whose acceptor stem sequences also differ significantly from that of tRNA^{Val}, can be converted to efficient valine acceptors by inserting a valine anticodon and replacing the G:U base pair in the acceptor stem of these tRNAs (*45*). The negative effects of G:U base pairs are strongly correlated with changes in helix structure in the vicinity of the 4:69 base pair, as monitored by ^{19}F NMR spectroscopy of 5-fluorouracil-substituted tRNA^{Val} (*45*), suggesting that maintaining regular A-type RNA helix geometry in the acceptor stem, at or near the 4:69 base pair, is important for proper recognition of tRNA^{Val} by valyl-tRNA synthetase.

Table 2: Aminoacylation Kinetics of *E. coli* tRNA^{Val} Mutants

tRNA	K_m (μM)	k_{cat} (s^{-1})	k_{cat}/K_m	relative k_{cat}/K_m
wild-type	1.4	9.0	6.4	(1.0)
discriminator base				
A73 → U73	2.5	4.9	2.0	0.30
→ G73	6.5	1.1	0.17	0.026
→ C73	2.3	6.7	2.9	0.45
variable pocket				
U17 → C17	1.2	8.8	7.4	1.1
G20 → A20	4.7	11.5	2.5	0.38
→ C20	6.0	11.2	1.9	0.29
→ U20	4.8	9.5	2.0	0.31
U59 → C59	1.2	7.2	6.0	0.93
→ G59	1.1	7.9	7.2	1.1
T-stem, central core, and variable loop				
G50:U64 → G50:C64	1.3	10.6	8.2	1.3
U47 → C47	1.1	8.3	7.5	1.2
[G45-(G10:C25)]				
→ [U45-(G10:C25)]	2.7	9.9	3.7	0.57
→ [A45-(G10:C25)]	3.8	11.9	3.1	0.49
G44 → A44	3.5	7.9	2.3	0.35
A26 → G26	3.6	10.4	2.9	0.45
G44 + A26 → A44 + G26	1.9	12.8	6.7	1.05

(4) Discriminator Base and 3′-CCA End. Substitution of G for the wild-type discriminator base, A73, of tRNA^{Val} results in a 40-fold reduction in aminoacylation efficiency (Table 2). The C73 and U73 variants are much more active, having k_{cat}/K_m values only 2− to 3-fold lower than that of wild-type tRNA^{Val} (Table 2). Evidently A73 is not an absolute requirement for the productive interaction of tRNA^{Val} with ValRS. Tamura et al. (*18*) also have investigated the role of the discriminator base of *E. coli* tRNA^{Val} in ValRS recognition. Although their results generally agree with ours, they reported the A73U mutant to be inactive, with an aminoacylation efficiency more than 3 orders of magnitude lower than that of wild-type tRNA^{Val}. Reasons for this discrepancy are not clear.

The identity of the discriminator base is known to affect the structure and stability of the acceptor helix of tRNA

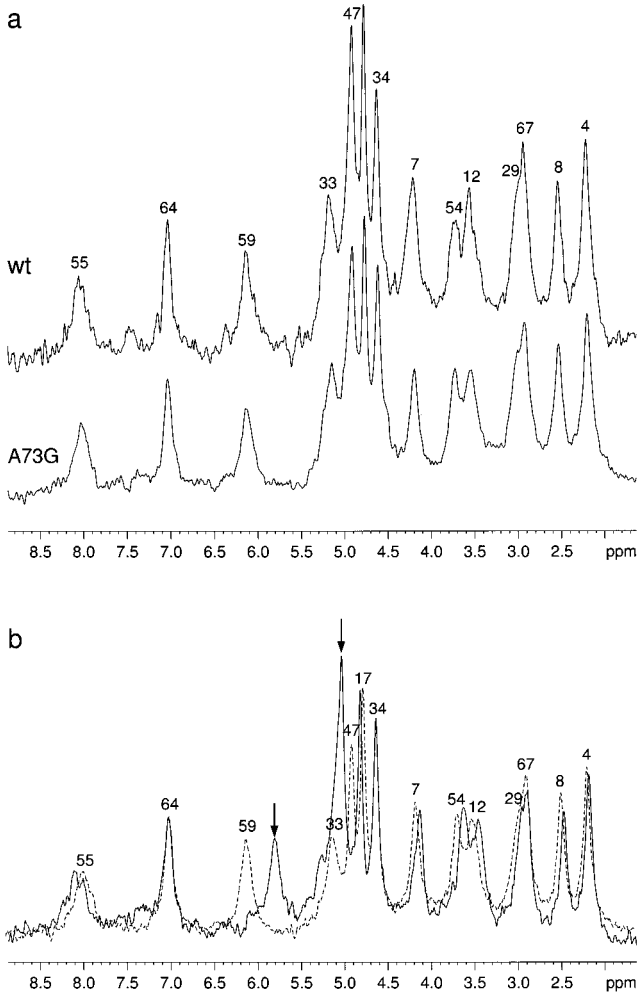

FIGURE 5: ^{19}F NMR spectra of 5-fluorouracil-substituted *E. coli* tRNA^{Val}: (a) (upper) wild-type tRNA^{Val}, (lower) mutant A73G; (b) (dashed line) wild-type tRNA^{Val}, (solid line) mutant G20C. Arrows indicate positions of ^{19}F resonances shifted in the spectrum of mutant G20C. Spectra were recorded at 47 °C.

(*46*−*48*). To determine whether changes in acceptor stem structure cause the observed decrease in aminoacylation efficiency of the A73G mutant (*45*), we have compared the ^{19}F NMR spectrum of FUra-substituted A73G tRNA^{Val} mutant with those of wild-type tRNA^{Val} and of the A73U mutant. The results clearly show that the spectra of wild-type tRNA^{Val} and of the A73G tRNA^{Val} mutant are identical (Figure 5a). In particular, there are no changes in the chemical shift positions of the three FUra residues in the acceptor stem, FU4, FU7, and FU67, which indicates that replacing A73 with G73 does not affect the overall structure of the tRNA or the local conformation of the acceptor stem. The ^{19}F spectrum of the A73U tRNA^{Val} mutant is also identical to that of wild-type tRNA^{Val} except for an additional peak due to the presence of FU73 (results not shown). These results suggest that guanosine at the discriminator position acts as an antideterminant for ValRS, either because it contains a functionality that blocks enzyme binding or because it lacks a functional group(s) necessary for proper recognition by ValRS. As we discussed previously (*49*), A, C, and U share common hydrogen bond donor/acceptor patterns that are absent in G and which may be essential for correct recognition of tRNA at the active site of the synthetase.

We had earlier shown that guanosine in place of the universally conserved 3′-terminal adenosine has a negative effect on the aminoacylation of tRNA^{Val}, reducing the charging efficiency more than 2 orders of magnitude due to a 300-fold decrease in k_{cat} (*49*). Valine tRNAs terminating in either 3′-cytidine or 3′-uridine retain almost full aminoacylation activity (*49*). Base substitutions for C74 and C75 have relatively little effect on the aminoacylation efficiency of tRNA^{Val}, except that the G75 variant exhibits a 185-fold decrease in k_{cat} (*49*).

(5) Variable Pocket, T-Stem, and Central Core. Nucleotides in the variable pocket (16, 17, 20, 59, and 60), the single-stranded region of tRNA where the T- and D-loops interact, as well as those involved in tertiary interactions in the central core are known to serve as synthetase recognition determinants for several tRNAs (e.g., *22*, *50*, *51*). In tRNA^{Val}, U17, U59, and C60 are not important for synthetase recognition since the conservative pyrimidine-pyrimidine substitutions U17C and U59C exhibit normal aminoacylation kinetics; the U59G mutant (Table 2) and the double mutant U59G;C60U (Tardif and Horowitz, unpublished) also are charged at the wild-type rate.

Converting G20 to any other nucleotide consistently reduces the aminoacylation efficiency 3−4-fold (Table 2). Although substitutions for G20 are not expected to affect tRNA structure because this nucleotide is not involved in stabilizing tertiary interactions, nucleotide substitutions at position 20 are known to produce structural changes in tRNA. Most pertinent to our results are the findings of Peterson and Uhlenbeck (*22*), who showed that replacing the wild-type U20 of *E. coli* tRNA^{Phe} reduces the lead cleavage rate. They also found that changing U20 to G20 introduces several additional lead cleavage sites into the tRNA. Both results indicate altered tRNA folding, which was attributed to the presence of three consecutive G residues in the D-loop of the U20G mutant (*22*).

The G18G19G20 sequence also is present in wild-type tRNA^{Val} (Figure 3), and ^{19}F NMR of FUra-containing tRNA^{Val} shows that mutations at position 20 produce structural changes (Figure 5b). Comparison of the ^{19}F NMR spectrum of the fluorine-substituted G20C variant (Figure 5b, solid line) with that of wild-type tRNA^{Val} (Figure 5b, dashed line) indicates that the two spectra are similar, but that in the spectrum of the G20C mutant, resonance FU59 is shifted 0.3 ppm upfield and FU47 shifts 0.2 ppm downfield, to overlap FU33. These structural changes in the variable pocket and the variable loop of the G20C variant of tRNA^{Val} make it difficult to determine whether the reduced catalytic efficiency of this tRNA is due to loss of a synthetase recognition determinant or the result of structural defects in the tRNA. To help resolve this uncertainty, we have examined the effects on valine acceptor activity of nucleotide substitutions at position 20 of a mutant *yeast* tRNA^{Phe}, tRNA^{Phe}(A36U;G4A), that readily accepts valine (*45*). Changing the nucleotide at position 20 of yeast tRNA^{Phe} was shown not to affect tRNA structure, as assessed by the rate of lead cleavage (*52*). If G20 is specifically recognized by ValRS, mutating G20 of yeast tRNA^{Phe}(A36U;G4A) should reduce valine acceptance. Aminoacylation kinetic experiments (results not shown) demonstrate that the aminoacylation efficiency (k_{cat}/K_m) for valine acceptance of tRNA^{Phe}(A36U;G4A) is 3 times that of the corresponding G20U variant, indi-

Table 3: Valine Acceptance of *E. coli* tRNA^{Phe} Mutants

tRNA	K_m (μM)	k_{cat} (s−1)	k_{cat}/K_m	relative k_{cat}/K_m
E. coli tRNA^{Val}				
tRNA^{Val}(UAC)(wild-type)	1.4	9.0	6.4	(1.0)
E. coli (tRNA)^{Phe}				
tRNA^{Phe}(GAA) (wild-type)	ND[b]	ND		
tRNA^{Phe}(GAC)	31.1	0.95	3.1×10^{-2}	5×10^{-3}
+G20	17.1	1.1	6.7×10^{-2}	1×10^{-2}
+G45	22.7	1.5	6.4×10^{-2}	1×10^{-2}
+G20 + G45	23.3	3.7	0.16	3×10^{-2}
tRNA^{Phe}(GAC)(G20)				
+A6:U67	−	−	0.17	3×10^{-2}
+C16	−	−	3.1×10^{-4}	4.8×10^{-5}
+C60	−	−	0.14	2×10^{-2}
+C16 + C60	−	−	2.5×10^{-4}	3.9×10^{-5}
tRNA^{Phe}(GAC)(G20)[a]	14.7	6.1	0.42	6×10^{-2}
+A3:U70[a]	−	−	0.63	0.10
+U4:A69[a]	−	−	0.56	9×10^{-2}
+G45[a]	8.0	9.0	1.13	0.18
tRNA^{Phe}(GAC)G20 (V-stem, V-loop)	4.3	10.1	2.3	0.36
tRNA^{Phe}(GAC)G20 + G45 (V-stem, V-loop)	1.5	9.2	6.1	0.95
tRNA^{Phe}(GAC)G20 + G45 (V-stem, F-loop)	1.8	9.9	5.5	0.86
tRNA^{Phe}(GAC)G20 + G45 (F-stem, V-loop)	16.5	3.8	0.23	4×10^{-2}

[a] The top three base pairs of the anticodon stem of tRNA^{Phe} (G27:C43+G28:C42+G29:C41) were replaced with the corresponding base pairs of tRNA^{Val} (C27:G43+C28:G42+U29:A41). [b] No detectable aminoacylation.

cating that G20 is a minor recognition determinant for ValRS.

Further mutational analysis (Table 2) shows that nucleotides in the T-stem, the variable loop, and central core are not important for synthetase recognition. Converting the G50:U64 wobble base pair in the T-stem to a G50:C64 Watson−Crick base pair, or substituting C47 for U47 in the variable loop, does not decrease valine accepting activity (Table 2). Substitution of A or U for G45 in the base triplet G45-G10-C25 reduces k_{cat}/K_m approximately 2.0-fold, compared to wild-type tRNA^{Val} (Table 2). Identity switch experiments with *E. coli* tRNA^{Phe}, described later, suggest that G45 is a minor synthetase recognition determinant. Mutations A26G and G44A in tRNA^{Val} result in moderate, 55−65%, reductions in aminoacylation efficiency (Table 2), due largely to a 2.5-fold increase in K_m. The double mutant A26G;G44A, which recapitulates the A:G tertiary base pair of wild-type tRNA^{Val}, with the location of the bases interchanged, is, however, as good a substrate for ValRS as wild-type tRNA^{Val} (Table 2). The reduced activity of the single mutants is probably due to structural changes in the tRNA. Bases at positions 26 and 44 form a purine-purine propeller twist tertiary interaction at the junction of the anticodon and D-stems. Peterson and Uhlenbeck (*22*) reported that single substitutions at positions 26 or 44 in *E. coli* tRNA^{Phe} result in misfolding of tRNA, as shown by the reduced rate of lead cleavage of the A26G and G44A mutants. Normal lead cleavage rate is restored in the double mutant, A26G;G44A (*22*), possibly because the propeller twist between G26 and A44 is isomorphic with that of the wild-type A26-G44.

Transplantation of tRNA^{Val} Recognition Determinants into E. coli tRNA^{Phe}. To test the completeness of the synthetase recognition set and to identify possible additional antideterminants, the known tRNA^{Val} identity elements, A35, C36, A73, and G20, were transferred into the framework of other, noncognate, tRNAs. In previous experiments we had shown that *E. coli* tRNA^{Ala}(UGC) and yeast tRNA^{Phe}(GAA) were readily transformed into efficient valine acceptors by introducing these identity nucleotides (where necessary) and removing G:U base pairs from the middle of the acceptor stem (*45*). Converting *E. coli* tRNA^{Phe}(GAA) into a good substrate for ValRS proved more difficult and permitted identification of additional synthetase recognition determinants.

Wild-type *E. coli* tRNA^{Phe}(GAA) is not aminoacylated with valine under standard experimental conditions (Table 3). The sequence of *E. coli* tRNA^{Phe} differs from that of *E. coli* tRNA^{Val} at 31 positions, including most of the acceptor stem, the entire anticodon stem, part of the anticodon loop, and part of the T-stem (see shaded areas in Figure 3a,c). Two of the four ValRS recognition nucleotides of tRNA^{Val} are missing, C36 and G20 (also G45). Introducing the valine anticodon into tRNA^{Phe} by converting A36 to C36 increases valine acceptance slightly (Table 3); however, the k_{cat}/K_m for this tRNA is still less than 1% that of wild-type tRNA^{Val}. Further substitution of G20 for U20 has little effect on activity; the tRNA remains a poor substrate for ValRS (Table 3). Additional mutations were introduced into different regions of tRNA^{Phe}(GAC)(G20) in attempts to increase valine-charging efficiency.

Because the G:C−rich nature of the acceptor stem of tRNA^{Phe} (Figure 3) may increase rigidity and interfere with productive interaction with ValRS, A:U base pairs were inserted at several positions in the acceptor stem. Introducing A3:U70 in place of G3:C:70, U4:A69 for C4:G69, or A6:U67 for G6:C67, however, improves aminoacylation efficiency with valine only a little (Table 3).

E. coli tRNA^{Val} and *E. coli* tRNA^{Phe} differ at four positions in the variable pocket (16, 17, 20, and 60) (Figure 3). As already mentioned, changing U20 to G20 in tRNA^{Phe}(GAC) has little effect on aminoacylation efficiency (Table 3). Similarly, substitution of C16 for U16, or C60 for U60, either singly or in combination with other mutations, fails to enhance valine acceptance in the tRNA^{Phe}(GAC)(G20) framework (Table 3). Valine and phenylalanine tRNAs also differ at position 45 (Figure 3). This nucleotide forms a base triple with the 10:25 base pair, which is G10:C25 in both tRNAs (Figure 3). Replacing the U45 of tRNA^{Phe}(GAC)-

(G20) with G45 increases k_{cat}/K_m 3-fold (relative k_{cat}/K_m = 0.18) (Table 3). The aminoacylation efficiency is still relatively low, but the results point to position 45 as a minor ValRS recognition element (see below).

The anticodon stem of tRNA^{Phe} is very G:C-rich, with four consecutive G:C base pairs (Figure 3). Because increasing the G:C content of the anticodon stem of tRNA^{Val} decreases the aminoacylation efficiency (Table 1), we examined effects of introducing A:U base pairs into the anticodon stem. Replacing the entire anticodon arm of *E. coli* tRNA^{Phe}(G20) with that of tRNA^{Val} raises the aminoacylation efficiency considerably. The resulting tRNA, tRNA^{Phe}(GAC)(G20)(V-stem,V-loop), has a relative k_{cat}/K_m of 0.36, due primarily to a 3-fold higher K_m compared with wild-type tRNA^{Val} (Table 3). This increase in valine-accepting activity is due only to the valine anticodon stem; the anticodon loop (outside the anticodon itself) makes no contribution to activity. When the valine anticodon loop alone is inserted into tRNA^{Phe}, the mutant tRNA is a poor substrate for ValRS, having a relative k_{cat}/K_m of only 0.04 (Table 3). On the other hand, the mutant tRNA^{Phe} with a Val-stem and a Phe-loop (except for the A36C mutation to introduce a valine anticodon) is a very good substrate, with a relative k_{cat}/K_m of 0.86 (Table 3). We have been unable to identify nucleotides in the anticodon stem responsible for the increase in activity. Individual or multiple base pair substitutions in the anticodon stem of tRNA^{Phe}(GAC)(G20) increase the aminoacylation efficiency to only 15−34% that of wild-type tRNA^{Val} (results not shown). All these variants have a much higher K_m (10−18-fold), which indicates that binding of the tRNA substrates by ValRS is severely affected.

Introducing G45, in place of U45, in mutants of tRNA^{Phe}-(GAC)(G20) containing a valine anticodon stem increases the valine acceptance activity to nearly wild-type levels, primarily by lowering the K_m (Table 3). These results confirm G45 as a minor ValRS recognition determinant.

Conclusion. Our study demonstrates that two anticodon bases, A35 and C36, are the major synthetase recognition determinants of *E. coli* tRNA^{Val}. In addition, guanosines at positions 20, in the variable pocket, and 45, in the tRNA central core, serve as minor recognition elements. Adenosine, cytidine, and uridine at the discriminator position (#73) are readily recognized by ValRS, but G73 acts as a negative determinant. Unlike most tRNAs, the amino acid acceptor helix of *E. coli* tRNA^{Val} has no synthetase recognition nucleotides, but regular A-type RNA helix geometry is essential, especially near the 4:69 base pair (*45*). Conformation of the anticodon stem of tRNA^{Val} also plays a role in ValRS recognition; mutant tRNAs with rigid, G:C-rich anticodon stems are poor valine acceptors. Nuclease mapping indicates that the nucleotide and structural determinants of ValRS recognition are all in contact with the synthetase.

ACKNOWLEDGMENT

We thank Olke Uhlenbeck (University of Colorado, Boulder) for the tRNA^{Phe}-containing plasmid and Shimin Li, Diane Shogren, and Daniel Spielbauer for technical assistance. This research benefited from the use of the 500-MHz NMR Biotechnology Instrumentation Facility at Iowa State University.

REFERENCES

1. Schulman, L. H. (1991) *Prog. Nucleic Acid Res. Mol. Biol. 41*, 23−57.
2. Giegé, R., Puglisi, J. D., and Florentz, C. (1993) *Prog. Nucleic Acid Res. Mol. Biol. 45* 129−205.
3. Giegé, R., Sissler, M., and Florentz, C. (1998) *Nucleic Acids Res. 26*, 5017−5035.
4. McClain, W. (1993) *J. Mol. Biol. 234*, 257−280.
5. Saks, M. E., Sampson, J. R., and Abelson, J. N. (1994) *Science 263*, 191−197.
6. Sekine, S., Nureki, O., Sakamoto, K., Niimi, T., Tateno, M., Gō, M., Kohno, T., Brisson, A., Lapointe, J., and Yokoyama, S. (1996) *J. Mol. Biol. 256*, 685−700.
7. Muramatsu, T., Nishikawa, K., Nemoto, F., Kuchino, Y., Nishimura, S., Miyazawa, T., and Yokoyama, S. (1988) *Nature 336*, 179−181.
8. Perret, V., Garcia, A., Grosjean, H., Ebel, J. P., Florentz, C., and Giegé, R. (1990) *Nature 344*, 787−789.
9. Rould, M. A., Perona, J. J., Söll, D., and Steitz, T. A. (1989) *Science 246*, 1135−1142.
10. Ruff, M., Krishnaswamy, S., Boeglin, M., Poterszmann, A., Mitchler, A., Podjarny, A., Rees, B., Thierry, J. C., and Moras, D. (1991) *Science 252*, 1682−1689.
11. Rudinger, J., Puglisi, J. D., Pütz, J., Schatz, D., Eckstein, F., Florentz, C., and Giegé, R. (1992) *Proc. Natl. Acad. Sci. U.S.A. 89*, 5882−5886.
12. McClain, W. H., and Foss, K. (1988) *Science 241*, 1804−1807.
13. Hou, Y. M., Westhof, E., and Giegé, R. (1993) *Proc. Natl. Acad. Sci. U.S.A. 90*, 6776−6780.
14. Hamann, C. S., and Hou, Y. M. (1997) *Biochemistry 36*, 7967−7972.
15. Schulman, L. H., and Pelka, H. (1988) *Science 242*, 765−768.
16. Derrick, W., Feiz, V., Chu, W.-C., and Horowitz, J. (1991) *FASEB J. 5*, A808.
17. Pallanck, L., and Schulman, L. H. (1991) *Proc. Natl. Acad. Sci. U.S.A. 88*, 3873−3876.
18. Tamura, K., Himeno, H., Ahahara, H., Hasegawa, T., and Shimizu, M. (1991) *Biochem. Biophys. Res. Commun. 177*, 619−623.
19. Horowitz, J., Chu, W.-C., Feiz, V., and Derrick, W. (1991) *14th International tRNA Workshop*, Rydzyna, Poland.
20. Zawadzki, V., and Gross, H. J. (1991) *Nucleic Acids Res. 19*, 1948−1955.
21. Chu, W.-C., and Horowitz, J. (1991) *Biochemistry 30*, 1655−1663.
22. Peterson, E. T., and Uhlenbeck, O. C. (1992) *Biochemistry 31*, 10380−10389.
23. Chu, W.-C., and Horowitz, J. (1989) *Nucleic Acids Res. 17*, 7241−7252.
24. Taylor, J. W., Ott, J., and Eckstein, F. (1985) *Nucleic Acids Res. 13*, 8765−8785.
25. Sanger, F., Coulson, A. R., Barrel, B. G., Smith, A. J. H., and Roe, B. A. (1980) *J. Mol. Biol. 143*, 161−178.
26. Sampson, J., and Uhlenbeck, O. C. (1988) *Proc. Natl. Acad. Sci. U.S.A. 83*, 1033−1037.
27. Liu, M., and Horowitz, J. (1993) *BioTechniques 15*, 264−266.
28. Schimmel, P. R., and Söll, D. (1979) *Annu. Rev. Biochem. 48*, 601−648.
29. Silberklang, M., Gillum, A. M., and RajBhandary, U. L. (1979) *Methods Enzymol. 59*, 58−109.
30. Derrick, W., and Horowitz, J. (1993) *Nucleic Acids Res. 21*, 4948−4953.
31. Donis-Keller, H., Maxam, A., and Gilbert, W. (1977) *Nucleic Acids Res. 4*, 2527−2538.
32. Kintanar, A., Yue, D., and Horowitz, J. (1994) *Biochimie, 76*, 1192−1204.
33. Yaniv, M., and Gros, F. (1969) *J. Mol. Biol. 44*, 1−15.
34. Shaw, D. (1976) in *Fourier Transform NMR Spectroscopy*, p 179, Elsevier, New York.
35. Witzel, H. (1963) *Prog. Nucleic Acid Res. Mol. Biol. 2*, 221−258.

36. Horowitz, J., Ou, C.-N., Ishaq, M., Ofengand, J., and Bierbaum, J. (1974) *J. Mol. Biol. 88*, 301−312.
37. Ofengand, J., Bierbaum, J., Horowitz, J., Ou, C.-N., and Ishaq, M. (1974) *J. Mol. Biol. 88*, 313−325.
38. Chu, W.-C., Feiz, V., Derrick, W. B., and Horowitz, J. (1992) *J. Mol. Biol. 227*, 1164−1172.
39. Chu, W.-C., Kintanar, A., and Horowitz, J. (1992) *J. Mol. Biol. 227*, 1173−1181.
40. Lowman, H. B., and Draper, D. E. (1985) *J. Biol. Chem. 261*, 5396−5403.
41. Schweizer, M. P., Olson, J. I., Nimai, D., Messner, A., Walkiu, I., and Grant, D. (1984) *Fed. Proc., Fed. Am. Soc. Exp. Biol. 43*, 2984−2986.
42. Schweizer, M. P., Olson, J. I., Stolk, J. A., Lee, Y.-C., Reeves, P. M., Perry, C., and De, N. (1989) *Biochim. Biophys. Acta 1008*, 293−300.
43. Chattapadhyay, R., Pelka, H., and Schulman, L. (1990) *Biochemistry 29*, 4263−4268.
44. Rould, M. A., Perona, J. J., and Steitz, T. A. (1991) *Nature 352*, 213−218.
45. Liu, M., Chu, W.-C., Liu, C.-H., and Horowitz, J. (1997) *Nucleic Acids Res. 25*, 4883−4890.
46. Lee, C. P., Mandal, N., Dyson, M. R., and RajBhandary, U. L. (1993) *Proc. Natl. Acad. Sci. U.S.A. 90*, 7149−7152.
47. Limmer, S., Hofmann, H.-P., Ott, G., and Sprinzl, M. (1993) *Proc. Natl. Acad. Sci. U.S.A. 90*, 6199−6202.
48. Puglisi, E. V., Puglisi, J. D., Williamson, J. R., and RajBhandary, U. L. (1994) *Proc. Natl. Acad. Sci. U.S.A. 91*, 11467−11471.
49. Liu, M., and Horowitz, J. (1994) *Proc. Natl. Acad. Sci. U.S.A. 91*, 10389−10393.
50. McClain, W. (1993) *J. Biol. Chem. 268*, 19398−19402.
51. Liu, H., Peterson, R., Kessler, J., and Musier-Forsyth, K. (1995) *Nucleic Acids Res.* 23, 165−169.
52. Behlen, L. S., Sampson, J. R., Direnzo, A. B., and Uhlenbeck, O. C. (1990) B*iochemistry 29*, 2515−2523.

BI990490B